Time-resolved infrared radiometry of NaCl crystals under shock compression between 17 and 43 GPa

Toshiyuki Ogura, Kazutaka G. Nakamura,* and Ken-ichi Kondo
Materials and Structures Laboratory, Tokyo Institute of Technology, R3-10, 4259 Nagatsuta, Yokohama 226-8503, Japan
(Received 15 June 2004; revised manuscript received 30 July 2004; published 22 October 2004)

Time-resolved infrared radiometry is performed on sodium chloride (NaCl) under shock compression between 17 and 43 GPa in order to measure shock temperatures. The infrared emission observed below 35 GPa reveals that the shock temperatures considerably less than the calculated continuum temperatures. Between 23 and 35 GPa, there is a mixed-phase region comprising high-temperature shear bands and a low-temperature bulk material involving luminescent sources.

DOI: 10.1103/PhysRevB.70.144110 PACS number(s): 62.50.+p, 78.47.+p

I. INTRODUCTION

Measurement of shock temperature is one of the most important issues in shock-wave research because of its significance to the experimental determination of the equation of state (EOS) and also its importance to geophysics and condensed matter physics.[1–6] Optical radiometry in the visible and near-ultraviolet regions is a well-developed technique and widely used in many laboratories to determine shock temperatures. However, the temperature range reliably determined by the method is limited in high temperatures above 1500 K. Furthermore, the radiometry in the visible region is strongly disturbed by nonthermal radiation such as triboluminescence and thermoluminescence from the shocked sample.[6,7]

Recently we delevoped time-resolved wideband radiometry in the visible and midinfrared (mid-IR) regions (0.6–13 μm), which enabled us to measure shock temperatures as low as 400 K.[8] In the mid-IR region, infrared emissions directly originate from thermal vibrations without any influence of nonequilibrium electrons. Radiance histories for shock compressed carbon tetrachloride were observed with approximately 10 ns time resolution and detemined the shock temperatures (680–1370 K) in the pressure range from 3.3 to 9.4 GPa.

In this paper, we measured temperatures of shock-loaded sodium chloride (NaCl) crystals over a pressure range between 17 and 43 GPa using time-resolved infrared radiometry. It is very important to determine the EOS of NaCl, because it has been used as a pressure scale.[9–12] Since shock-compression data generally include a thermal-pressure component due to the temperature rise, an accurate measurement of shock temperatures for NaCl would allow a more detailed understanding of the nature of the shock-compression state and some thermodynamic behavior to determine the accuracy of the NaCl pressure scale. However, the reported shock temperature data below 30 GPa (Refs. 2–5) were obtained by radiometry in the visible region and nonthermal radiation and hot shear bands were superimposed in the visible region and obscured the thermal emission from the bulk sample.[2,6,7]

II. EXPERIMENT

A planar shock wave is generated in NaCl by impacting with a copper plate at a velocity of 1.7–3.7 km/s. The copper plate embedded to a projectile is accelerated by a two-stage light-gas gun with a 20-mm bore.[8] The shock compression state in NaCl is determined by the impedance matching method using the impact velocity, which is measured with a magnetoflyer method[13] within an error of 2%, and known EOS (Ref. 14) of Cu and NaCl. The obtained shock velocity in NaCl agrees with that estimated from the temporal profile of IR emission for a high-strain case within experimental errors ($\leqslant$8%). The obtained pressures were between 17 and 43 GPa. The NaCl sample with thickness of 3–7.5 mm and 20 mm diameter is glued to the driver plate and mounted with its [100] or [111] crystallographic axis parallel to the propagation direction of the shock wave. In order to screen out possible emissions generated at the interface between the driver plate and the NaCl sample, a copper film is coated onto one side of the sample surface.[6]

The emission from NaCl during propagation of shock waves was recorded with two different types of radiometer and oscilloscope.[8] A radiometer consists of three beam splitters and four detectors, each with an interference filter and a Si or InGaAs photodiode. IR emission in the range of 9.0–13 μm was detected through a bandpass filter with a HgCdTe photodiode (a liquid-nitrogen cooling type, Kolmar Tech. Inc. KV-104). The output voltage from the IR radiometer, I_∞, is calibrated to the blackbody temperature between 400 and 1400 K with a blackbody furnace before every shot. The visible emissions were also measured using four detectors sensitive to wavelengths of 601, 806, 1107, and 1618 nm, with 50–100 nm [full width at half maximum (FWHM)] bandwidth. The radiometer is calibrated with a tungsten standard lamp (Optronic Laboratories Inc., model 550C) to the absolute radiance. Each radiometer has a temporal resolution of 3 ns. The details are described in elsewhere.[8]

III. RESULTS AND DISCUSSION

Figure 1(a) shows the time-resolved IR radiance histories at shock pressure of 21 GPa. Similar emission profiles are obtained for all other shock pressures tested in this work. Shock wave enters in the NaCl sample at time $t=0$ on the abscissa and emerges from the free surface about $t=1.4$ μs later.

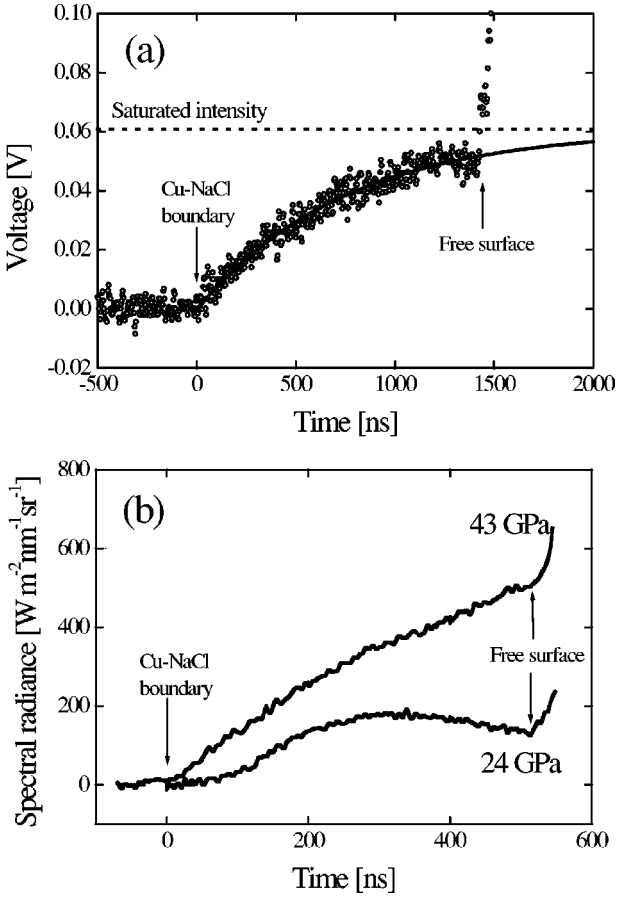

FIG. 1. Typical temporal changes of emission for various shock pressures. Shock wave propagated parallel to [100] crystallographic axis. (a) 9–13 μm for 21 GPa (○) and curve fitting of Eq. (1) of $a_S = 1.66$ cm^{-1} and $I_\infty = 0.0608$ V. The corresponding temperature is 540 ± 40 K. Sample thickness is 7.5 mm. (b) 1.1 μm for 24 and 43 GPa from 4.2-mm-thick samples. Arrows indicate the instance when shock wave reached at Cu-NaCl boundaries and free surfaces.

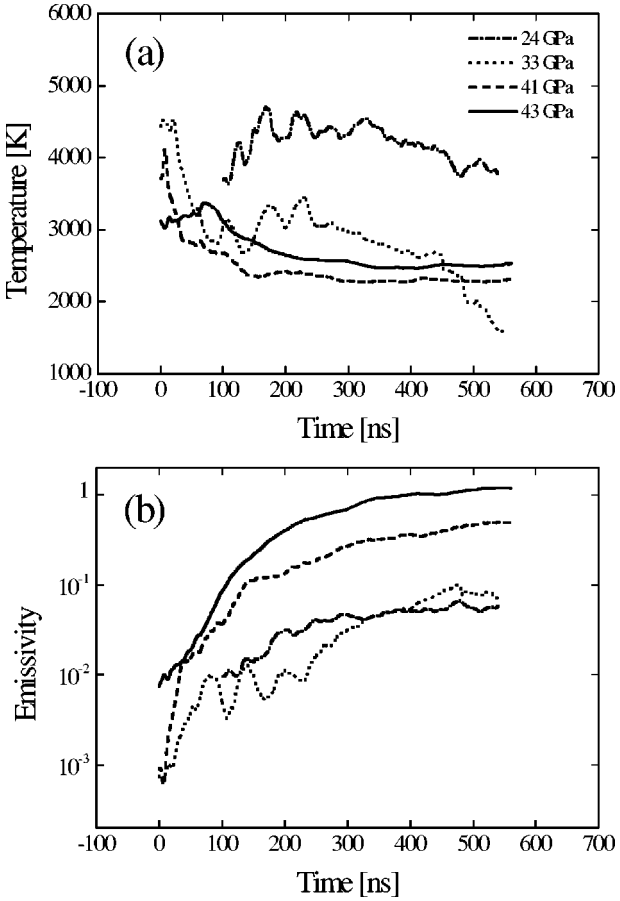

FIG. 2. Temporal changes of shock temperature (a) and emissivity (b) obtained from 0.6–1.6-μm emissions at pressure between 24 and 43 GPa.

The shock temperature was obtained from the temporal profile of IR emission using a formula[15,16] integrated over the bandwidth of 9.0–13 μm:

$$I(t) = I_\infty[1 - e^{-a_S(U_S - u_p)t}][1 + Re^{-a_S(U_S - u_p)t}]e^{-a_u(d - U_S t)}, \quad (1)$$

where a_S and a_U are the effective absorption coefficients of NaCl behind and ahead of the shock front, U_S and u_p are the shock and the particle velocities, d is the initial thickness of NaCl, and R is the reflectivity of the interface between the NaCl sample and Cu film. The parameter I_∞ represents the intensity of IR emission from a blackbody. The value of a_U is nearly zero for infrared emission shorter than 13 μm. The reflectivity of the interface is measured in this work to be 0.948 for the 9.0–13-μm emission. A least-squares fit of the emission data to Eq. (1) determines the unknown parameters a_S and I_∞ to be $a_S = 1.66$ cm^{-1} and $I_\infty = 0.0608$ V. The result is shown by the solid curve in Fig. 1(a), corresponding to the shock temperature of 547 ± 40 K with an effective emissivity of 0.85 at the arrival time of the shock wave at the free surface. The shock temperatures obtained form IR radiometry for other pressures are shown in Fig. 3, below.

Figure 1(b) shows the temporal profiles of 1.1-μm emissions at 24 and 43 GPa. It is possible to represent the temporal profile at 43 GPa by Eq. (1) but not the profile at 24 GPa. The temporal changes at 33 and 41 GPa not shown here have similar general shapes as the cases at 24 and 43 GPa in Fig. 1(b), respectively. Namely, below 33 GPa, the emissions are peaked at 200–300 ns. Such a behavior is not expected from an equilibrium radiation by greybody or semitransparent body. The profiles for 0.6-, 0.8-, and 1.6-μm emissions have a similar pressure dependence as the case for 1.1 μm. No emission is detected in the 0.6–1.6-μm wavelength range at pressures below 24 GPa.

In order to compare with previously reported color temperatures,[2–4,6] we tentatively estimated the efective-color temperature from the visible and near-IR data, although this color temperatures may not represent actual temperatures. We derived temporal changes of the effective-color temperature and emissivity by applying a least-squares method to the Plank's law of radiation to fit these four channels emission data[17] at selected time. Figures 2(a) and 2(b) show the resulting temporal profiles of the color temperature and emissivity derived from visivle and near-IR data at four shock pressures. In the cases of 24 and 33 GPa, the color temperature [Fig. 2(a)] gradually decreases after 150 ns and the emissivity [Fig. 2(b)] increases to 0.05. Hence, the emissions are

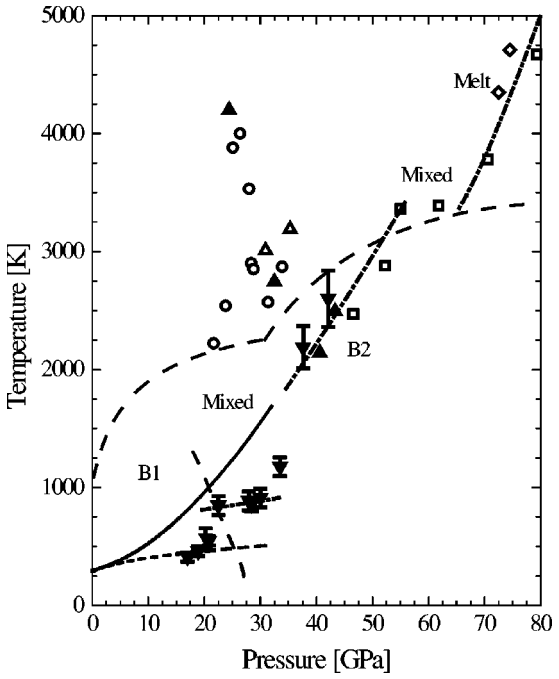

FIG. 3. Shock temperatures of NaCl determined in this work along with the data in the literature below 80 GPa. Solid triangles are the present measurements of 0.6–1.6 μm (▲) and 9–13 μm (▼) emissions. Open squares, lozenges, triangles, and circles are after Kormer (Ref. 2), Schmitt and Ahrens (Ref. 3), Kondo and Ahrens (Ref. 4), and Schmitt *et al.* (Ref. 5), respectively. Bold dashed lines denote the *B*1-*B*2 phase boundary after Li and Jeanloz (Ref. 18) and the solid-liquid boundary after Boehler *et al.* (Ref. 19). Solid line and dashed line denote the calculated Hugoniot temperature by Fritz *et al.* (Ref. 12) and the calculated temperature along isentropic compression, respectively.

associated with a small radiating volume. It suggests that the emissions originate not from an equilibrium radiation by homogeneous greybody or semitransparent body[15,16] but from hot shear bands or luminescence from various color centers generated under shock compression.[2–5] In contrast, the temperature profiles at 41 and 43 GPa quickly decrease from the instantaneous value of 4000 K at a few ten's of nanoseconds, followed by approaching to a constant value between 2100 and 2500 K after 200 ns, and the emissivity profiles approach to unity, which approximately corresponds to the absorption coefficient of the IR emission. Such apparent features of temporal changes in the color temperature and emissivity may not represent actural changes and may be due to disproportionate uncertainties. The uncertainty in the effective temperature is very large ($\sim$50%) at early times ($\leqslant$100 ns) due to the very low emissivity ($<$0.1) and becomes small ($\leqslant$10%) at late times. The uncertainty of emissivity is also large ($\sim$50%) at early times. The color temperatures are obtained by averaging the temporal data after 150 ns (shown in Fig. 3): 4200±2000 K, 2745±800 K, 2142±190 K, and 2494±230 K at 24.4 GPa, 32.5 GPa, 40.6 GPa, and 43.3 GPa, respectively. The obtained color temperatures, which are affected by triboluminescence and thermoluminescence, are in good agreement with the published data for color temperatures.[2–4,6]

Figure 3 shows comparisons between the present shock temperature data of NaCl (between 17 and 43 GPa) and the previous measurements and calculations. It is clearly shown that the temperature data exhibit different characteristics depending on the pressure: region I below 23 GPa, region II between 23 and 35 GPa, and region III above 35 GPa.

Region I corresponds to the low-pressure phase (*B*1: rocksalt structure). In this region, the temperatures based on the IR emission data lie significantly below the continuum shock temperatures.[12] The 0.6–1.6-μm emissions could not be detected in this region. The actual temperature along the Hugoinot line may be lower than those obtained by Fritz's model calculation.

Region II corresponds to the mixed-phase region of *B*1 and *B*2 (high-pressure phase of CsCl structure) phases. The discontinuous increase of IR temperatures at 23 GPa in Fig. 3 is in good agreement with the phase boundary determined from the static high-pressure and high-temperature experimental data,[18] but lower than the reported value at 26.4 GPa from the conventional Hugoniot measurement.[12] The temperatures from the present IR measurements are lower than the calculated continuum temperature (solid curve) and gradually increase from 800 to 900 K. On the other hand, the temperatures from the 0.6–1.6-μm emissions (indicated by the solid triangle) are distinctly higher than the calculated continuum temperature values and agree with the values in the literatures.[4,5] There is at present not enough information to conclude if this difference is due to the emissions from thermal hot bands or luminescent sources. However, it is significant to note that such large differences are only seen in the mixed-phase range and that the temperatures are much higher than the melting curve[19] in Fig. 3.

Region III at pressures higher than 35 GPa corresponds to the high-pressure phase of *B*2 (CsCl structure). The measured temperatures here are in good agreement with extrapolations of the previous result[2,3] (indicated by open squares) to lower pressures. There is also a good agreement in temperatures obtained from the 0.6–1.6-μm emission (solid triangle) and the 9–13-μm emission (inverted solid triangle) data, respectively. It shows that the system can achieve thermodynamic equilibrium within shock duration time.

In conclusion, the present work shows low thermal emission from NaCl crystal below 35 GPa under shock loading and shock temperatures considerably less than the calculated continuum temperatures. Namely, between 23 and 35 GPa, there is a mixed-phase region comprising high-temperature shear bands and a low-temperature bulk material involving luminescent sources.

ACKNOWLEDGMENTS

We thank M. F. Nicol of UNLV and F. H. Ree of LLNL for helpful discussions. This work was supported by Core Research for Evolutional Science and Technology (CREST) program of Japan Science and Technology Corporation (JST) and by a Grant-in-Aid for Scientific Research (A), No. 15204041.

*Author to whom correspondence should be addressed. Electronic address: nakamura@msl.titech.ac.jp

[1] J. M. Brown, J. Appl. Phys. **86**, 5801 (1999).
[2] S. B. Kormer, Sov. Phys. Usp. **11**, 229 (1968).
[3] D. R. Schmitt and T. J. Ahrens, Geophys. Res. Lett. **10**, 1077 (1983).
[4] K. Kondo and T. J. Ahrens, Phys. Chem. Miner. **9**, 173 (1983).
[5] D. R. Schmitt, T. J. Ahrens, and B. Svendsen, J. Appl. Phys. **63**, 99 (1988).
[6] K. Kondo, T. J. Ahrens, and A. Sawaoka, J. Appl. Phys. **54**, 4382 (1983).
[7] P. J. Brannon, C. H. Konrad, R. W. Morris, E. D. Jones, and J. R. Asay, J. Appl. Phys. **54**, 6374 (1983).
[8] O. V. Fat'yanov, T. Ogura, M. F. Nicol, K. G. Nakamura, and K. Kondo, Appl. Phys. Lett. **77**, 960 (2000).
[9] D. R. Decker, J. Appl. Phys. **42**, 3239 (1971).
[10] G. J. Piermarini, S. B. Block, D. Barnett, and R. A. Forman, J. Appl. Phys. **46**, 2774 (1975).
[11] H. K. Mao, P. M. Bell, J. W. Shaner, and D. J. Steinberg, J. Appl. Phys. **49**, 3276 (1978).
[12] J. N. Fritz, S. P. Marsh, W. J. Carter, and R. G. McQueen, *Accurate Characterization of the High Pressure Environment*, NBS Spec. Publ. No. 326 (U.S. GPO, Washington D.C., 1968), p. 201.
[13] *LASL Shock Hugoniot Data*, compiled by S. P. Marsh (University of California, Berkeley, 1980).
[14] K. Kondo, A. Sawaoka, and S. Saito, Rev. Sci. Instrum. **48**, 1581 (1977).
[15] H. Sugiura, K. Kondo, and A. Sawaoka, J. Appl. Phys. **53**, 4512 (1982).
[16] M. B. Boslough, J. Appl. Phys. **58**, 3394 (1985).
[17] G. A. Lyzenga and T. J. Ahrens, Rev. Sci. Instrum. **50**, 1421 (1979).
[18] X. Li and R. Jeanloz, Phys. Rev. B **36**, 474 (1987).
[19] R. Boehler, M. Ross, and D. B. Boercker, Phys. Rev. Lett. **78**, 4589 (1997).